Prepared for submission to JCAP

Photon paths around hyperbolic topological black holes in conformal Weyl gravity

Marco Olivares[a] **Constanza Osses**[b] **J. R. Villanueva**[b]

[a] *Facultad de Ingeniería, Universidad Diego Portales, Avenida Ejército Libertador 441, Casilla 298–V, Santiago, Chile.*

[b] *Instituto de Física y Astronomía, Universidad de Valparaíso, Avenida Gran Bretaña 1111, Casilla 5030, Playa Ancha, Valparaíso, Chile*

E-mail: marco.olivaresr@mail.udp.cl, conyosses@gmail.com, jose.villanuevalob@uv.cl

Abstract. In this research we find analytical solutions to the null geodesics around a hyperbolic topolical black hole in the conformal Weyl gravity. Exact expressions for the horizons are found, and they depend on the cosmological constant and the coupling constants of the conformal Weyl gravity. The angular motion is examined qualitatively by means of an effective potential; quantitatively, the equation of motion is solved in terms of $\wp$-Weierstraß elliptic function. Thus, we find the deflection angle for photons without using any approximation, which is a novel result for this topology.

Keywords: Modified Gravity; Black Holes; Elliptic Functions.

arXiv:1608.02979v1 [gr-qc] 9 Aug 2016

[1] Corresponding author.

Contents

1 Introduction: Conformal Weyl gravity and null geodesics **1**

2 Hyperbolic topological black hole in conformal Weyl gravity **2**
2.1 Allowed orbits 5
2.2 Bending of light 7

3 Summary **8**

1 Introduction: Conformal Weyl gravity and null geodesics

The conformal Weyl gravity (CWG) theory is a fourth order field theory introduced by Weyl to unify gravity and electromagnetism [1–4], and can be obtained from the conformally invariant action

$$I_W = 2\,\alpha \int \mathrm{d}^4x\,\sqrt{-g}\,\left[R_{\mu\nu}\,R^{\mu\nu} - \frac{1}{3}\left(R^{\mu}_{\mu}\right)^2\right], \tag{1.1}$$

where α is a dimensionless parameter which is chosen to be positive if (1.1) is a positive definite Euclidean action. The vacuum field equations associated with this action are solved by the static, spherically symmetric line element given by [5–9]

$$\mathrm{d}\tilde{s}^2 = -B(\tilde{r})\,\mathrm{d}\tilde{t}^2 + \frac{\mathrm{d}\tilde{r}^2}{B(\tilde{r})} + \tilde{r}^2(\mathrm{d}\Theta^2 + \sin^2\Theta\,\mathrm{d}\Phi^2), \tag{1.2}$$

where the set of coordinates $(\tilde{t}, \tilde{r}, \Theta, \Phi)$ are defined in the range $-\infty < \tilde{t} < \infty$, $\tilde{r} \geq 0$, $0 \leq \Theta \leq \pi$, $0 \leq \Phi \leq 2\pi$, and the lapse function $B(\tilde{r})$ is given by

$$B(\tilde{r}) = 1 - \frac{\beta(2 - 3\beta\,\tilde{\gamma})}{\tilde{r}} - 3\beta\,\tilde{\gamma} + \tilde{\gamma}\tilde{r} - \tilde{k}\tilde{r}^2. \tag{1.3}$$

Here β, $\tilde{k}$ and $\tilde{\gamma}$ are positive constants associated with the central mass, cosmological constant and the measurements of the departure of the Weyl theory from the Einstein - de Sitter, respectively. Clearly, taking the limit $\tilde{\gamma} = 0 = \tilde{k}$ recovers the Schwarzschild case so that we can identify $\beta = M$, and thus work with dimensionless quantities by making the following identifications:

$$\frac{\mathrm{d}\tilde{s}}{M} \to \mathrm{d}S, \quad \frac{\tilde{t}}{M} \to T, \quad \frac{\tilde{r}}{M} \to \tilde{R}, \quad M\,\tilde{\gamma} \to \Gamma, \quad M^2\,\tilde{k} \to K.$$

Therefore, the metric and the lapse function become

$$\mathrm{d}S^2 = -B(\tilde{R})\,\mathrm{d}T^2 + \frac{\mathrm{d}\tilde{R}^2}{B(\tilde{R})} + \tilde{R}^2(\mathrm{d}\Theta^2 + \sin^2\Theta\,\mathrm{d}\Phi^2), \tag{1.4}$$

and

$$B(\tilde{R}) = 1 - \frac{(2 - 3\Gamma)}{\tilde{R}} - 3\Gamma + \Gamma\tilde{R} - K\tilde{R}^2, \tag{1.5}$$

respectively. Study of the basis and properties, together with applications of the motion of massive and massless particles in this geometry can be found, for example, in [10–20],

and can be obtained using the standard Lagrange procedure [21–28], which make it possible to associate a Lagrangian $\mathcal{L}$ with the metric and then obtain the equation of motion from Lagrange's equations

$$\dot{\Pi}_q - \frac{\partial \mathcal{L}}{\partial q} = 0, \tag{1.6}$$

where $\Pi_q = \partial\mathcal{L}/\partial\dot{q}$ are the conjugate momenta to the coordinate q, and the dot denotes a derivative with respect to the affine parameter τ along the geodesic. In the next sections, following the procedure performed by Klemm [29], but taking into account that the metric (1.4) is dimensionless, we permorm an analytical continuation to obtain a non-trivial topology associated with black holes in CWG, and then we study the null geodesics on these manifolds.

2 Hyperbolic topological black hole in conformal Weyl gravity

In order to obtain a class of topological black hole, we perform the analytical continuation suggested by [29]:

$$\mathrm{d}S \to i\,\mathrm{d}s, \quad \Gamma \to \gamma, \quad K \to -k, \quad T \to -t, \quad \tilde{R} \to -r, \quad \Phi \to \phi, \quad \Theta \to i\,\theta, \tag{2.1}$$

so Eqs. (1.4)-(1.5) yield to

$$\mathrm{d}s^2 = -B(r)\,\mathrm{d}t^2 + \frac{\mathrm{d}r^2}{B(r)} + r^2(\mathrm{d}\theta^2 + \sinh^2\theta\,\mathrm{d}\phi^2), \tag{2.2}$$

$$B(r) = -1 - \frac{(2-3\gamma)}{r} + 3\gamma + \gamma r - kr^2, \tag{2.3}$$

and the Lagrangian reads

$$\mathcal{L} = \frac{1}{2}B(r)\,\dot{t}^2 + \frac{\dot{r}^2}{2B(r)} + \frac{r^2}{2}(\dot{\theta}^2 + \sinh^2\theta\,\dot{\phi}^2). \tag{2.4}$$

Clearly, the metric induced on the spacelike surface of constants t and r is the standard metric of hyperbolic 2-space $\mathbb{H}^2$, $\mathrm{d}\sigma^2 = r^2(\mathrm{d}\theta^2 + \sinh^2\theta\,\mathrm{d}\phi^2)$, which has a constant negative curvature and is not compact.

From the hyperbolic lapse function (2.3), it is possible to construct the cubic polynomial

$$p_3(r) = -\frac{rB(r)}{k} = r^3 - \frac{\gamma}{k}r^2 + \frac{(1-3\gamma)}{k}r + \frac{(2-3\gamma)}{k}, \tag{2.5}$$

which gives us the locations of the horizons (if there are any). In fact, defining $r_w = \gamma/3k$ and then making the change of variable:

$$r = x + r_w, \tag{2.6}$$

we write the cubic polynomial in its canonical form

$$p_3(x) = x^3 - \eta_2\,x - \eta_3, \tag{2.7}$$

where the coefficients are given by

$$\eta_2 = 3\,r_w^2 + 9\,r_w - \frac{1}{k}, \tag{2.8}$$

$$\eta_3 = 2\,r_w^3 + 9\,r_w^2 + \left(9 - \frac{1}{k}\right)\,r_w - \frac{2}{k}. \tag{2.9}$$

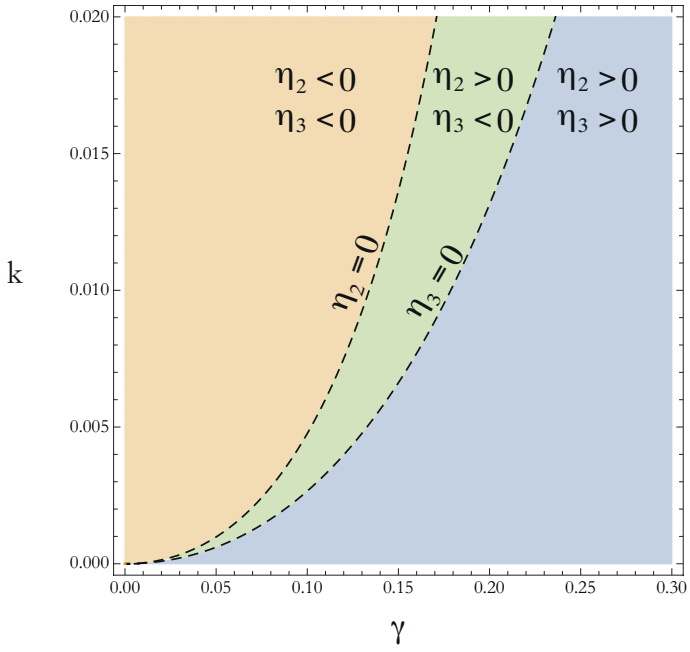

Figure 1. This region plot shows the sign of the cubic parameters of the polynomial (2.7), η_2 and η_3, on the k-γ plane. The region in which $\eta_2 < 0$ and $\eta_3 < 0$ does not allow real solution to the equation $p_3(x) = 0$.

Obviously, the nature of the coefficients depends on the combination of the pair (γ, k). In Fig. 1 three different regions appear with the possible choice of the sign of η_2 and η_3 on the k-γ plane. In the region between $\gamma = 0$ and $\eta_2 = 0$, the roots of the polynomial $p_3(x)$ satisfy the equation $x^3 + |\eta_2|\, x + |\eta_3| = 0$, so there is no real solution for $x > 0$, and thus we dismiss this case. On the other hand, another way to obtain information about the roots can be inferred from the cubic discriminant $\Delta_c = 27\eta_3^2 - 4\eta_2^3$. Thus, if $\Delta_c < 0$, there is one real negative root and a complex pair of the roots, and this represents a naked singularity; if $\Delta_c > 0$, there are three different real roots, two positive and one negative, which looks similar to the SdS spacetime with an event and cosmological horizons. Finally, if $\Delta_c = 0$, there are three real roots, a negative one plus a degenerate positive root, and this represents the extreme case. Thus, for example, if we assume that γ is small, then the coefficient η_3 is negative, and therefore the discriminant of the polynomial is positive, $\Delta_c > 0$.

Denoting

$$R = \sqrt{\frac{|\eta_2|}{3}}, \quad \varphi = \frac{1}{3}\arccos\left(\frac{\eta_3}{R^3}\right), \tag{2.10}$$

we can find the expression for the event horizon, r_+, the cosmological horizon, r_{++}, and the negative root (without physical meaning), r_n, and they take the form

$$r_+ = r_w + \frac{R}{2}(\cos\varphi - \sqrt{3}\sin\varphi), \tag{2.11}$$

$$r_{++} = r_w + R\cos\varphi, \tag{2.12}$$

$$r_n = r_w - \frac{R}{2}(\cos\varphi + \sqrt{3}\sin\varphi). \tag{2.13}$$

Conversely, the hyperbolic metric (2.2) admits the following Killing vector field:

- the *time-like Killing vector* $\xi = \partial_t$ is related to the stationarity of the metric. The conserved quantity is given by

$$g_{\mu\nu}\,\xi^{\mu}\,u^{\nu} = -B(r)\,\dot{t} = -\sqrt{E} \tag{2.14}$$

where E is a constant of motion that cannot be associated with the total energy of the test particle because this metric is not asymptotically flat.

- the most general *space-like Killing vector* is given by

$$\vec{\xi} = (A\,\cos\phi + B\,\sin\phi)\,\partial_\theta + [C - \coth\theta\,(A\,\cos\phi + B\,\sin\phi)]\,\partial_\phi, \tag{2.15}$$

where A, B and C are arbitrary constants. It is easy to see that it is a linear combination of the three Killing vectors

$$\chi_1 = \partial_\phi, \quad \chi_2 = -\coth\theta\,\sin\phi\,\partial_\phi + \cos\phi\,\partial_\theta, \quad \chi_3 = \coth\theta\,\cos\phi\,\partial_\phi + \sin\phi\,\partial_\theta,$$

which are the angular momentum operators for this spacetime. The conserved quantities are given by

$$g_{\alpha\beta}\,\chi_1^{\alpha}\,u^{\beta} = r^2\,\sinh^2\theta\,\dot{\phi} = L_1, \tag{2.16}$$
$$g_{\alpha\beta}\,\chi_2^{\alpha}\,u^{\beta} = r^2\,(\cos\phi\,\dot{\theta} - \sinh\theta\,\cosh\theta\,\sin\phi\,\dot{\phi}) = L_2, \tag{2.17}$$
$$g_{\alpha\beta}\,\chi_3^{\alpha}\,u^{\beta} = r^2\,(\sin\phi\,\dot{\theta} + \sinh\theta\,\cosh\theta\,\cos\phi\,\dot{\phi}) = L_3, \tag{2.18}$$

where L_1, L_2 and L_3 are constants associated with the angular momentum of the particles and a dot represents a derivative with respect to an affine parameter τ along the geodesic. With no lack of generality, we focus our attention on the invariant plane $\phi = \pi/2$, so $\dot{\phi} = 0$, and therefore we have that $L_1 = L_2 = 0$, $L_3 \equiv J$, where J is the total angular momentum. This last assumption implies that Eqs. (2.16–2.18) reduce to an unique angular equation of motion:

$$\dot{\theta} = \frac{J}{r^2}. \tag{2.19}$$

Using Eqs. (2.14) and (2.19), and taking into account that the Lagrangian associated with the motion of photons is null, $\mathcal{L} = 0$, it is easy to obtain the radial equation of motion

$$\dot{r}^2 = E - V(r), \tag{2.20}$$

where $V(r)$ is the effective potential which satisfies the relation

$$\frac{V(r)}{E} \equiv \mathcal{V}(r) = b^2\,\frac{B(r)}{r^2}, \tag{2.21}$$

and $b = J/\sqrt{E}$ is the impact parameter. This last point is relevant for the radial motion, since $V(r) \propto b^2 = 0$; the familiar and well studied relation $\dot{r} = \pm\sqrt{E}$ is recovered. In its essence, the motion presents the same feature know in other spacetimes (see for example [21–23]). On the other hand, by combining Eqs. (2.19) and (2.20), we obtain the radial–polar equation

$$\left(\frac{dr}{d\theta}\right)^2 = \frac{r^4}{b^2}\,[1 - \mathcal{V}(r)]\,. \tag{2.22}$$

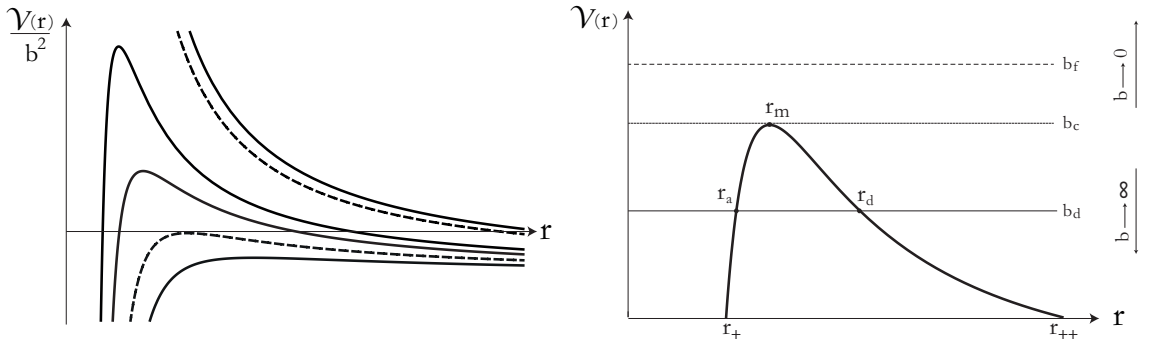

Figure 2. Left panel: Evolution of the conformal effective potential, per unit of b^2, for photons in Weyl's gravity as a function of the Weyl parameter γ with a fixed value of the cosmological parameter $k = 0.05$. The upper dashed line corresponds to the curve with $\gamma = \gamma_c$ while the lower dashed line corresponds to the extreme topological black hole, for which the relation $V_m = 0$ is satisfied. Right panel: Typical effective potential with three general regions for the motion of photons: deflection zone, in which the impact parameter poses a value between $[b_c < b \equiv b_d < \infty]$, asymptotic zone, in which the impact parameter has the value $b = b_c$, and a capture zone in which the impact parameter has a value between $[0 < b \equiv b_f < b_c]$.

In FIG.2 we have plotted the conformal effective potential (per unit of b^2) as a function of the radial coordinate, for a fixed value of the cosmological parameter $k = 0.05$. The evolution of the curves was made in terms of the Weyl's parameter γ. Thus, as with Einstein's black hole, the position of the maximum r_m is independent of k and is thus only a function of γ:

$$r_m = 3\left(\frac{\gamma_c}{\gamma} - 1\right), \tag{2.23}$$

where $\gamma_c = 2/3$. At this point the impact parameter assumes the critical value

$$b_c = \frac{1}{\sqrt{k_{ext} - k}}, \tag{2.24}$$

where $k_{ext} = (1 - \gamma)/r_m^2$. In the same figure, the upper dashed line represents the effective potential for γ_c, which implies that $r_m = 0$ and $V(r_m) \equiv V_m \to \infty$, whereas on the lower dashed line the relation $k = k_{ext}$ is satisfied, which represents the *extreme case* for which $V_m = 0$. Note that the latter condition implies that $b_c \to \infty$. With this in mind, we focus our attention on the family of potential lies between these two well defined curves. The next subsection is devoted to analyzing the effective potential qualitatively in terms of the impact parameter.

2.1 Allowed orbits

As we have mentioned, under the assumption that $\gamma < \gamma_c$ and $k < k_{ext}$, massless particles can perform different kinds of orbits, which depend, in essence, on their impact parameter. In this way, based on the classification of b shown in the left panel of Figure 2, we present a brief qualitative description of the angular motions permitted for photons in hyperbolic topological black holes in conformal Weyl gravity.

- *Unbounded trajectories (capture zone)*: If $0 < b \equiv b_f < b_c$, the incident photons fall inexorably to one of the two horizons, depending on the initial conditions placed on

their velocity. The cross section, σ, in this geometry is [30]

$$\sigma = \pi\, b_c^2 = \frac{\pi}{k_{ext} - k}. \tag{2.25}$$

- *Critical trajectories*: If $b = b_c$, photons can stay in the unstable inner circular orbit of radius r_m. Therefore, the photons that arrive from the initial distance r_i ($r_+ < r_i < r_m$, or $r_m < r_i < r_{++}$) can asymptotically fall to a circle of radius r_m. The proper period in such an orbit is given by

$$T_\tau = \frac{2\,\pi\, r_m^2}{J} = \frac{18\,\pi}{J}\left(\frac{\gamma_c}{\gamma} - 1\right)^2, \tag{2.26}$$

which is independent of k, whereas the coordinate period depends on k and γ as

$$T_t = 2\,\pi\, b_c = \frac{2\,\pi}{\sqrt{k_{ext} - k}}. \tag{2.27}$$

- *Deflection Zone.* If $b_c < b = b_d < \infty$, the photons come from a finite distance r_i ($r_+ < r_i < r_m$ for orbits of the first kind or $r_m < r_i < r_{++}$ for orbits of the second kind) to a turning point r_t (which is the solution to the equation $\mathcal{V}(r_t) = 1$), and then return to one of the two horizons. Therefore, by defining

$$R_W = \frac{\gamma\,\mathcal{B}^2}{3}, \quad \bar{R} = \sqrt{\frac{\varrho_2}{3}}, \quad \zeta = \frac{1}{3}\arccos\sqrt{\frac{27\,\varrho_3^2}{\varrho_2^3}}, \tag{2.28}$$

where the cubic coefficients are given by

$$\varrho_2 = 3\,\gamma_c^2\,\mathcal{B}^2\left[\gamma^2\,\mathcal{B}^2 + 3\left(\frac{3 - r_m}{3 + r_m}\right)\right], \tag{2.29}$$

and

$$\varrho_3 = \gamma_c^2\,\mathcal{B}^2\left[\gamma_c\,\gamma^3\,\mathcal{B}^4 + \frac{6\,(3 - r_m)}{(3 + r_m)^2}\,\mathcal{B}^2 - \frac{18\,r_m}{3 + r_m}\right], \tag{2.30}$$

and $\mathcal{B}$ is the *anomalous impact parameter* given by

$$\mathcal{B} = \frac{b}{\sqrt{1 + k\,b^2}}, \tag{2.31}$$

these solutions are given explicitly through the following equations:

$$r_1 = R_W - \frac{\bar{R}}{2}\left(\sqrt{3}\sin\zeta + \cos\zeta\right), \tag{2.32}$$

$$r_a = R_W + \frac{\bar{R}}{2}\left(\sqrt{3}\sin\zeta - \cos\zeta\right), \tag{2.33}$$

$$r_d = R_W + \bar{R}\cos\zeta. \tag{2.34}$$

Notice that if the condition $\varrho_2^3 > 27\varrho_3^2$ is assumed, it is not difficult to show that the preceding solutions satisfy $r_1 < 0 < r_a < r_d$. Also note that, as has been pointed out by Cruz et al. [22], since k is very small, only when $b \sim k^{-1/2}$ is the net effect of $\mathcal{B}$ relevant in (2.31). Also, if the product $k\,b^2 \gg 1$ (or $b \to \infty$), then $\mathcal{B} \sim k^{-1/2}$ in such way that $\varrho_2 \to \eta_2$ and $\varrho_3 \to \eta_3$ (cf. Eqs. (2.8)–(2.29) and Eqs. (2.9)–(2.30)). Therefore, as expected, the identities $r_a(\infty, \gamma, k) = r_+$ and $r_d(\infty, \gamma, k) = r_{++}$ can be proven in a few steps [15].

In order to obtain the analytical expression for the orbit in which the photons are moving, we perform an integration of Eq. (2.22), resulting in

$$r(\theta) = |x_1| \pm \frac{1}{4\wp(\kappa\,\theta;\, g_2, g_3) - \alpha_1/3}, \qquad \text{if} \quad b_c < b < \infty, \tag{2.35}$$

$$r(\theta) = \frac{1}{4\wp(\kappa\,\theta + \omega_0;\, g_2, g_3) - \alpha_1/3}, \qquad \text{if} \quad 0 < b \leq b_c, \tag{2.36}$$

where $\wp(x; g_2, g_3)$ is the $\wp$-Weierstraß elliptic function, whose Weierstraß invariants are given by

$$g_2 = \frac{1}{4}\left(\frac{\alpha_1^2}{3} - \beta_1^2\right), \qquad g_3 = \frac{1}{16}\left(\frac{\alpha_1\beta_1^2}{3} - \frac{2}{27}\alpha_1^3 - \gamma_1^3\right), \tag{2.37}$$

whereas the constants appearing in Eqs. (2.35-2.37) are given explicitly by

$$\kappa = \frac{\sqrt{x_1\,x_2\,x_3}}{\mathcal{B}}, \qquad \alpha_1 = \frac{1}{x_1} + \frac{1}{x_2} + \frac{1}{x_3}$$

$$\beta_1 = \left[\frac{1}{x_1\,x_2} + \frac{1}{x_1\,x_3} + \frac{1}{x_2\,x_3}\right]^{1/2}, \qquad \gamma_1 = \frac{1}{[x_1\,x_2\,x_3]^{1/3}}.$$

Also, the plus and minus sign in Eq. (2.35) corresponds to orbits of the first kind ($r \geq r_d$) and orbits of the second kind ($r \leq r_a$), respectively (see right panel of Fig. 2), and the values of x_j ($j = 1, 2, 3$) depend on the region where the motion is performed as well as the type of the orbit. Table 2.1 summarizes the values used in Equations (2.35) and (2.36), which depend on the value of the impact parameter, whereas in Fig. 3 the trajectories obtained from Equation (2.36) are shown, i.e., for photons with $b \leq b_c$.

Table 1. Quantities used in Eqs. (2.35) and (2.36) to obtain the trajectories of the photons in the exterior geometry of a hyperbolic topological black hole in conformal Weyl gravity.

Type of orbit	Range for r	Range for b	x_1	x_2	x_3	ω
First kind	$r > r_d$	$b_c < b < \infty$	r_d	$r_d - r_a$	$r_d - r_1$	–
Second kind	$r < r_a$	$b_c < b < \infty$	$-r_a$	$r_d - r_a$	$-(r_a - r_1)$	–
Critical FK	$r > r_m$	$b = b_c$	r_1	$-r_d$	$-r_a$	$\wp^{-1}(\frac{\alpha_1}{12})$
Critical SK	$r < r_m$	$b = b_c$	r_1	$-r_d$	$-r_a$	0
Unbounded	$r > r_+$	$0 < b < b_c$	r_1	$-r_d$	$-r_a$	0

2.2 Bending of light

As an application of the preceding section, specifically of the polar equation (2.35) for the orbit of the first kind covered by the light, it is possible to study how this is deflected due to presence of the black hole, which, for the sake of simplicity, is placed at the origin of a system of coordinate O. Therefore, in order to obtain a full description, we employ the exact method outlined by Villanueva & Olivares [15] instead of the Rindler–Ishak method performed in other works [31–35].

Suppose that in $t = t_0$ photons are emitted with impact parameter $b_c < b < \infty$ by a source placed at the position given by $(r_i, \theta_i) = (r_\star, \theta_\star)$ with respect to O. Therefore, photons traveling in the exterior spacetime of a hyperbolic topological black hole are deflected

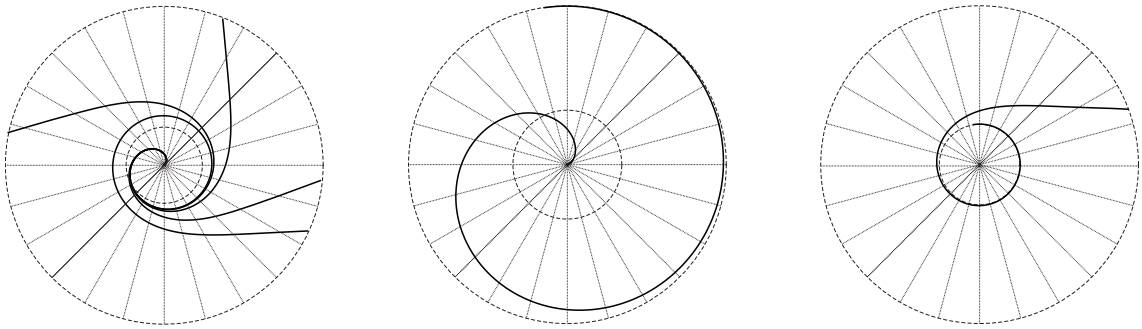

Figure 3. Plots referring to Eq. (2.35) in a cut of the $\phi = \pi/2$-invariant plane of the hyperbolic topological Weyl black hole. LEFT PANEL: Unbounded trajectory for massless particles with $b < b_c$. The fall to the cosmological horizon or event horizon depends on the initial direction of their motion. MIDDLE PANEL: Critical trajectory of the first kind, in which $r_i < r_m$ and $b = b_c$. Photons can asymptotically fall to a circle of radius r_m or fall to the event horizon. RIGHT PANEL: Critical trajectory of the second kind, in which $r_i > r_m$ and $b = b_c$. Photons can asymptotically fall to a circle of radius r_m or fall to the cosmological horizon.

in such way they reach the turning point r_d given by Eq. (2.33), and then are received by an observer placed at an other position on the manifold $(r_\oplus, -\theta_\oplus)$ (see left-top panel of Fig. 4). Based on the same plot, it is not difficult to prove that

$$\widehat{\alpha} = |\theta_\bigstar| + |\theta_\oplus| - \pi; \tag{2.38}$$

therefore, by combining Eq. (2.35) with Eq. (2.38), the deflection angle becomes

$$\widehat{\alpha} = \frac{1}{\kappa}\left(\left|\wp^{-1}\left[\frac{1}{4(r_\bigstar - r_d)} + \frac{\alpha_1}{12}\right]\right| + \left|\wp^{-1}\left[\frac{1}{4(r_\oplus - r_d)} + \frac{\alpha_1}{12}\right]\right|\right) - \pi, \tag{2.39}$$

where $\wp^{-1}$ is the inverse $\wp$-Weierstraß function [36–40]. In botom left panel of Fig. 4, the deflection angle as a function of b^{-2} is plotted, and it shows that there is a special value at which the deflection angle vanishes. This means that the scattering of photons by a hyperbolic topological black hole can be attractive or repulsive (with respect to the black hole), depending on the influence of the event horizon or the cosmological horizon (see top and bottom right panel of Fig. 4).

3 Summary

In this research, we have studied some aspects of the topology for a hyperbolic topological black hole in the conformal Weyl gravity, the metric of which is given by Eq. (2.3). In this sense, we analyze the existence of the event horizon, r_+, and the cosmological horizon, r_{++}, as a function of the cosmological parameter k, and the Weyl parameter, γ, as shown in Fig. 1, and we obtain their analytical expression in terms of these parameters. Also, the Killing vector fields are obtained and therefore four conserved quantities appear, showing the stationarity and the rotational invariance of the metric. These symmetries reduce our study to an unidimensional equivalent problem on an invariant plane, which is choosen to be $\phi = \pi/2$. A quick view of the equations of motion show us that the radial motion of photons presents the same features performed in the standard conformal Weyl gravity [15],

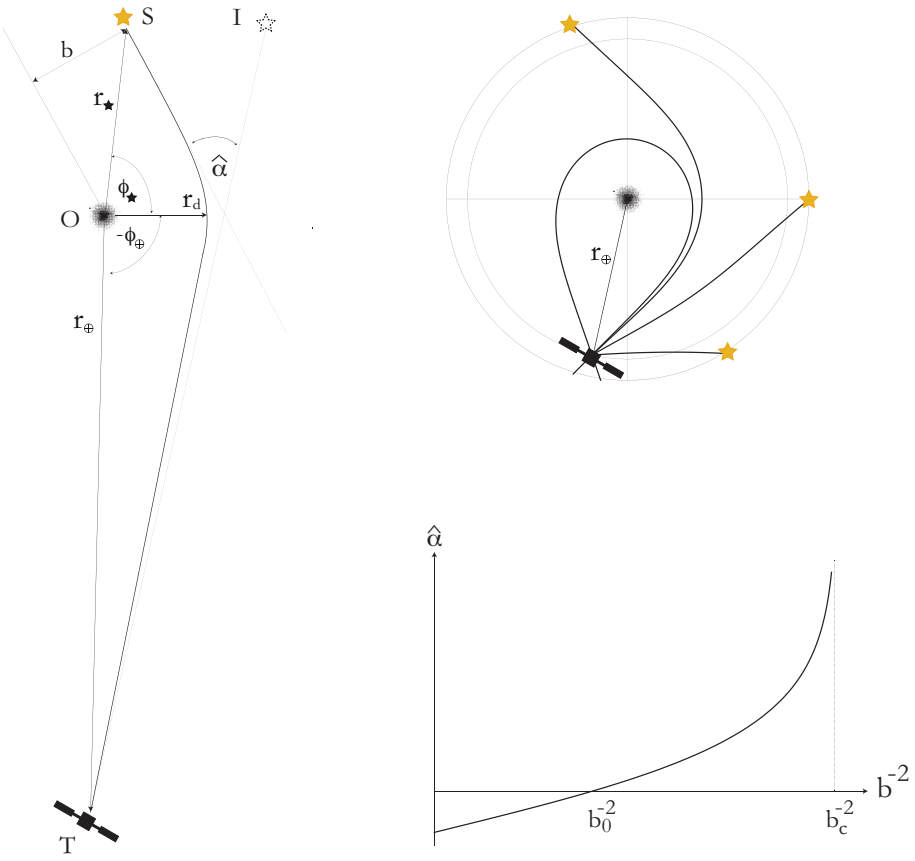

Figure 4. Gravitational lensing from a hyperbolic topological black hole in conformal Weyl gravity. LEFT: Light with impact parameter b from the source S at $(r_\star, \theta_\star)$ bends at the lens O and arrives at the observer T at $(r_\oplus, -\theta_\oplus)$, who then sees the image I; TOP RIGHT: Trajectories for different values of the impact parameter as observed at T; BOTTOM RIGHT: The angle of deflection $\widehat{\alpha}$ as a function of b^{-2}. There is a critical value of the impact parameter b_0, for which the deflection angle vanishes and thus the bending of light can be attractive or repulsive. Also, the deflection angle tends to be infinite at the critical impact parameter b_c.

and therefore, in the same way as Einstein's black holes, photons cross the horizons in a finite proper time, whereas in an external system, the photons fall asymptotically to the horizons.

The angular motion was first studied qualitatively by means of an analysis of the effective potential as a function of the radial distance for different values of the impact parameter b (see Fig. 2). Therefore, under the condition $\gamma < \gamma_c$ and $k < k_{ext}$, this analysis shows the existence of a maximum for which photons with $b = b_c = (k_{ext} - k)^{-1/2}$ either fall to one of the horizons or tend asymptotically to an unstable circular orbit at r_m. Also, we note that the existence of the unstable circular orbit depends on the parameter γ, which is a novel result because in the standard conformal Weyl gravity only depends on the mass M [15]. For this reason, the proper period also depends on the Weyl parameter γ, whereas the coordinate period, as we expect, depends on γ and k. However, if the value of the impact parameter is $0 < b < b_c$, then photons fall inexorably to one of the horizons. Finally, when the impact parameter is $b = b_d$ so $b_c < b_d < \infty$, the trajectory is deflected in such way that for $r \leq r_a$; then r_a corresponds to an apoastron distance, or for $r \geq r_d$, the distance r_d corresponds to a

periastron distance. The exact calculation of both distances, r_a and r_d, makes it possible to verify that at the limit $b \to \infty$, the consistency relations $r_a \to r_+$ and $r_d \to r_{++}$ are satisfied.

For the quantitative analysis of the motion, we employ an integration of the general equation of motion (2.19) in such way that we obtain two general equations for the trajectories described for the photons: unbounded and critical trajectories ($0 < b \leq b_c$) are described by Eq. (2.35) and are shown in Fig. 3, whereas orbits of the first and the second kind are described by Eq.(2.36), in which case the orbits are bounded.

As an application of our previous results, we obtain an exact expression in terms of the inverse $\wp$-Weierstraß function, for the deflection angle $\widehat{\alpha}$ experienced by photons emitted with impact parameter b_d by a source with coordinates $(r_\bigstar, \theta_\bigstar)$ with respect to the black hole system (which acts as a gravitational lens). The photons are then received by an observer at $(r_\bigoplus, -\theta_\bigoplus)$ (see left top panel of Fig. 4). One important and interesting result is the physical type of the deflection experienced by the massless particles. Depending on the value of the impact parameters this can be either attractive or repulsive with respect to the black hole. This feature is better appreciated in the bottom left panel of Fig. 4, in which the deflection angle $\widehat{\alpha}$ vanishes at a specific value of the impact parameter b_0.

Acknowledgments

We wish to thank A. Comas for the graphs and plots and V. Motta for the useful conversation. This work was funded by the Comisión Nacional de Investigación Científica y Tecnológica through FONDECYT Grant No 11130695.

References

[1] H. Weyl, *Zur gravitationstheorie*, Annalen der Phys. **54** (1917) 117.

[2] H. Weyl, *Reine infinitesimalgeometrie*, Math. Zeitschr. **2** (1918) 384.

[3] H. Weyl, *Gravitation und electrizität*, Sitz. Ber. Preuss. Ak. Wiss. (1918) 465.

[4] R. Bach, *Zur Weylschen relativitätstheorie und der Weylschen erweiterung des krümmenstensorsbegriffs*, Math. Zeitschr. **9** (1921) 110.

[5] R.J. Riegart, *Birkhoff's theorem in conformal gravity*, Phys. Rev. Lett. **53** (1984) 315.

[6] P.D. Mennheim and D. Kazanas, *Exact vacuum solution to conformal Weyl gravity and galactic rotation curves*, Astrophys. J. **342** (1989) 635.

[7] D.Kazanas and P.D. Mennheim, *General structure of the gravitational equations of motion in conformal Weyl gravity*, Astrophys. J. Suppl. **76** (1991) 431.

[8] P.D. Mennheim and D. Kazanas, *Solutions to the Reissner-Nordström, Kerr, and Kerr-Newman problems in fourth-order conformal Weyl gravity*, Phys. Rev. D **44** (1991) 417.

[9] P.D. Mennheim and D. Kazanas, *Newtonian limit of conformal gravity and the lack of necessity of the second order Poisson equation*, Gen. Rel. Grav. **26** (1994) 337.

[10] A. Edery and M. B. Paranjape, *Classical tests for Weyl gravity: Deflection of light and time delay*, Phys. Rev. D **58** (1998) 024011.

[11] S. Pireaux, *Light deflection in Weyl gravity: Critical distances for photon paths.*, Class. Quant. Grav. **21** (2004) 1897.

[12] S. Pireaux, *Light deflection in Weyl gravity: Constraints on the linear parameter*, Class. Quant. Grav. **21** (2004) 4317.

[13] J. Sultana and D. Kazanas, *Bending of light in conformal Weyl gravity*, Phys. Rev. D **81** (2010) 127502.

[14] J. Sultana, D. Kazanas and J.L. Said, *Conformal Weyl gravity and perihelion precession*, Phys. Rev. D **86** (2012) 084008.

[15] J.R. Villanueva and M. Olivares, *On the null trajectories in conformal Weyl gravity*, JCAP **06** (2013) 040.

[16] J.L. Said, J. Sultana and K.Z. Adami, *Gravitomagnetic effects in conformal gravity*, Phys. Rev. D **88** (2013) 087504.

[17] J. Sultana, *The Sagnac effect in conformal Weyl gravity*, Gen. Relativ. Gravit. **46** (2014) 1710.

[18] J. L. Said, J. Sultana and K. Z. Adami, *Exact Static Cylindrical Solution to Conformal Weyl Gravity*, 2012 Phys. Rev. D **85** 104054.

[19] H. Lu, Y. Pang, C. N. Pope, and J. F. Vazquez-Poritz, *AdS and Lifshitz Black Holes in Conformal and Einstein-Weyl Gravities*, 2012 Phys. Rev. D **86** 044011.

[20] F. Payandeh and M. Fathi, *Spherical Solutions due to the Exterior Geometry of a Charged Weyl Black Hole*, 2012 Int. J. Theor. Phys. **51** 2227.

[21] S. Chandrasekhar, *The Mathematical Theory of Black Holes*, Oxford University Press, New York, 1983.

[22] N. Cruz, M. Olivares and J. R. Villanueva, *The geodesic structure of the Schwarzschild anti-de Sitter Black Hole*, 2005 Class. Quant. Grav. **22** 1167-1190.

[23] B. Shutz, *A First Course in General Relativity*, Cambridge University Press, 1990.

[24] M. Olivares, J. Saavedra, C. Leiva and J. R. Villanueva, *Motion of charged particles on the Reissner-Nordström (Anti)-de Sitter black holes*, 2011 Mod. Phys. Lett. A **26** 2923.

[25] M. J. Jaklitsch , C. Hellaby and D. R. Matravers, *Particle motion in the spherically symmetric vacuum solution with positive cosmological constant*, 1989 Gen. Rel. Grav. **21**, 941.

[26] J. R. Villanueva, J. Saavedra, M. Olivares and N. Cruz, *Photons motion in charged anti de Sitter black holes*, 2013 Astrophys. Space Sci. **344**, 437-446.

[27] M. Halilsoy, O. Gurtug and S. Habib Mazharimousavi, *Rindler modified Schwarzschild geodesics* Gen. Rel. Grav. **45**, 2363 (2013) [arXiv:1312.5574 [gr-qc]].

[28] C. Leiva, J. Saavedra and J.R. Villanueva, *The geodesic structure of the Schwarzschild black holes in gravitys Rainbow*, Mod. Phys. Lett. A 24, 1443-1451 (2009) [arXiv:0808.2601 [gr-qc]].

[29] D. Klemm, *Topological black holes in Weyl conformal gravity*, Class. Quantum Grav. **15** (1998) 3195.

[30] R. Wald, *General Relativity*, University of Chicago Press, Chicago, 1984.

[31] W. Rindler and M. Ishak, *Contribution of the cosmological constant to the relativistic bending of light revisited*, 2007 Phys. Rev. D **76** 043006.

[32] M. Ishak and W. Rindler, *The Relevance of the Cosmological Constant for Lensing*, 2010 Gen. Rel. Grav. **42** 2247-2268.

[33] M. Ishak, W. Rindler and J. Dossett, *More on Lensing by a Cosmological Constant*, 2010 Mon. Not. Roy. Astron. Soc. **403**, 2152.

[34] F. Finelli, M. Galaverni and A. Gruppuso, *Light Bending as a Probe of the Nature of Dark Energy*, 2007 Phys. Rev. D **75** 043003.

[35] A. Bhattacharya, A. Panchenko, M. Scalia, C. Cattani and K. K. Nandi, *Light bending in the galactic halo by Rindler-Ishak method*, 2010 JCAP **1009** 004.

[36] P. F. Byrd and M. D. Friedman, *Handbook of Elliptic Integrals for Engineers and Scientists*, 2nd ed., rev. Berlin: Springer-Verlag (1971).

[37] H. Hancock, *Lectures on the theory of elliptic functions*, Dover publications Inc. New York (1958).

[38] J. V. Armitage and W. F. Eberlein, Elliptic functions, London Mathematical Society Student Texts. (No. 67), Cambridge University Press (2006).

[39] K. Meyer, *Jacobi elliptic functions from a dynamical systems point of view*, Amer. Math. Monthly **108** (2001) 729.

[40] I. S. Gradshteyn and I. M. Ryzhik, *Table of integrals, series, and products*, Academic Press. (2007).